Orthogonal Multicarrier Division Multiple Access for Multipoint-to-Multipoint Networks

Wenxun Qiu, *Member, IEEE,* Poramate Tarasak, and Hlaing Minn, *Senior Member, IEEE*

***Abstract*—We develop new transmission schemes for multipoint-to-multipoint (M2M) networks which, unlike the existing approaches, address duplexing/multiplexing and multiple access jointly and possess true M2M characteristics in the physical layer. In the proposed schemes, all forward and reverse links of the M2M network share the overall spectrum concurrently in an orthogonal frequency division manner. This provides increased degrees of freedom and enhanced diversity in scheduling and resource allocation, thus leading to performance enhancement. We first discuss practical implementation issues. Next, we develop our proposed schemes for both centralized and distributed access scenarios. Under the centralized access, we illustrate advantages of the proposed approach for M2M networks using a scheduling algorithm and provide a closed-form analytical throughput upper-bound. Next, we extend the proposed approach to multicasting and present a new scheduling strategy and its closed-form analytical approximate throughput expression. Under the distributed access, we develop a generalized multi-channel carrier sensing multiple access/collision avoidance scheme for M2M networks and propose a new scheme which exploits local channel information. Closed-form analytical throughput expressions for a specific scenario are also presented. Simulation results corroborate substantial performance gains of the proposed schemes over the conventional schemes in both centralized and random access scenarios.**

***Index Terms*—Multipoint-to-multipoint, multicast, multiplexing, multichannel CSMA/CA, scheduling.**

I. Introduction

MULTIPOINT-TO-MULTIPOINT (M2M) network is one of the emerging wireless systems and finds many applications: multimedia multi-point file sharing/streaming [1], real-time social networks [2], virtual collaborative environment [3], etc. Conventionally, M2M communications are implemented by higher layer protocols [4]. In the physical layer, they comprise several point-to-point (P2P) systems (e.g., [5]) or point-to-multipoint (P2M) systems (e.g., [6]). Thus, the physical layer transmissions in the existing M2M systems are not true M2M. Essentially, we can view them as time division duplexing/multiplexing (TDD/TDM) or frequency division duplexing/multiplexing (FDD/FDM) with frequency division multiple access (FDMA), orthogonal frequency division multiple access (OFDMA) or time division multiple access (TDMA) in the physical layer. The isolation of system resources among different links limits degrees of freedom and dimensionality in resource allocation, thus constraining performance potentials.

M2M systems can be designed under centralized/scheduled access or distributed/random access. The system with scheduled access is contention-free and has a central node to schedule different links and to allocate the system resources. The distributed access is a contention based communication scheme [7], [8], where no node takes the role of a central entity for managing the accesses, and collisions occur with non-zero probability. Under centralized access, the use of OFDM-TDMA serves in the form of multiple P2P systems while the use of OFDMA provides the structure of multiple P2M systems. For the distributed access scenario, single channel OFDM with CSMA protocol could provide M2M communications in the form of multiple P2P systems while multi-channel CSMA could form a limited-scale true M2M in the physical layer. The existing multi-channel CSMA schemes [9]–[11] offer lower collision rate than the single channel counterpart, but none of them have been applied under a true M2M communication setup in the physical layer. Recently, [12] has presented a multi-channel CSMA / collision avoidance (CA) based on OFDMA which can achieve even lower collision probability and better channel utilization. However, it was proposed for the uplink of P2M networks.

In this paper, we propose a new type of transmission scheme for M2M networks termed as orthogonal multicarrier division multiple access (MDMA). The underlying concept of the proposed scheme is that with proper synchronization among all the nodes the overall spectrum is shared concurrently by all forward and reverse links of the M2M network in an orthogonal frequency division manner. This provides increased degrees of freedom and enhanced diversity, thus yielding performance improvement in scheduling and resource allocation. The contributions of this paper are described below:

i) We propose a new transmission scheme, named MDMA, for M2M networks which has several unique features not available in the existing M2M systems. First, it addresses multiple access and duplexing/multiplexing jointly and without restrictions within the available spectrum of the system, which translates the M2M system into the one with enlarged degrees of freedom, resource dimensionality, and diversity gain, yielding overall system performance enhancement. Second, it provides true M2M communications in the physical layer which can substantially improve throughput performance of the M2M

Manuscript received September 17, 2012; revised March 6 and May 14, 2013. The editor coordinating the review of this paper and approving it for publication was H. Arslan.

W. Qiu is with Texas Instruments Inc, Dallas, TX, USA (e-mail: w-qiu@ti.com).

H. Minn is with the University of Texas at Dallas, Richardson, TX, USA (e-mail: hlaing.minn@utdallas.edu).

P. Tarasak was with the Institute for Infocomm Research, Singapore (e-mail: pom_uvic@yahoo.ca).

Some parts or concepts of this paper were presented at IEEE ICC 2012 [13] and Globecom 2012 [29].

Digital Object Identifier 10.1109/TCOMM.2013.13.120704

network. Third, it facilitates channel state information (CSI) acquisition with less delay and overhead because all links share the same spectral range all the time and the forward and reverse link channels are reciprocal.

ii) For M2M networks with centralized access, we apply a scheduling scheme to illustrate substantial throughput gains of the proposed MDMA over FDM-OFDMA and TDM-OFDMA. We derive a closed-form analytical throughput upper bound of the proposed MDMA with the centralized access.

iii) We extend the proposed MDMA to M2M multicasting environments and present a centralized scheduling strategy. Under such environment and scheduling, MDMA substantially outperforms FDM-OFDMA and TDM-OFDMA. We also provide a closed-form analytical approximate throughput expression of the proposed MDMA multicasting scheme.

iv) For M2M networks with distributed access, we generalize an existing multi-channel CSMA proposed for the uplink of P2M networks to M2M networks, yielding lower collision probability and higher channel utilization than the existing single channel CSMA/CA based M2M scheme. In addition, we propose a new multi-channel CSMA/CA for M2M networks which exploits local CSI at each node to improve throughput further. We also provide closed-form throughput expressions under a specific condition for the both proposed schemes. We assess several M2M distributed access schemes in terms of collision probability, idle probability, channel utilization rate, and the overall performance metric of average total throughput where the proposed scheme with local CSI exploitation achieves significant gains over the other schemes.

The paper is organized as follows. In Section II, we describe the basic idea of MDMA and its implementation issues. In Section III, the centralized MDMA scheduled access in M2M networks is discussed and an extension to scheduling of multicast M2M system is proposed. The distributed access for MDMA is discussed in Section IV. Simulation results are given in Section V and conclusions are provided in Section VI.

II. Orthogonal Multicarrier Division Multiple Access for M2M systems

A. Basic Idea

In [13]–[15], orthogonal multicarrier division duplexing (MDD) is proposed for P2P communications. The forward and reverse links of MDD share the spectrum without inserting guard bands, which brings more degrees of freedom. In MDD, any two nodes synchronize with each other so that all subcarriers belonging to both links are orthogonal. For each transceiver, the subcarrier range of the discrete Fourier transform (DFT) covers both transmitting subcarriers and receiving subcarriers and any subcarrier can be assigned to either link. By sharing the whole frequency band, MDD can have better diversity performance than FDD and can adapt to channel variations more closely than TDD. An implementation of the above simultaneous transmission and reception of MDD is reported in [16]. Our recent work in [13] optimizes subcarrier partitioning of MDD and shows that duplexing in terms of interleaved subchannels composing of contiguous subcarriers is better and more robust against inter-carrier interferences.

In this paper, we extend this idea to M2M networks where each node connects to all the other nodes of the same M2M network. The proposed MDMA can be also viewed as multicarrier division multiplexing (MDM) with OFDMA, which can be applied to both P2M and M2M networks, but we focus on the latter. The underlying idea of the proposed scheme is that the whole frequency band is shared by all the nodes within the system concurrently without any large guard band. To achieve this, all the nodes within the system synchronize with each other so that subcarriers of all the links among those nodes are mutually orthogonal. For each node, the subcarrier range of DFT should cover the subcarriers of all the transmit and receive links. The signals from all the links should be aligned at OFDM symbol level for all the nodes through synchronization process (small mismatch can be solved by the cyclic prefix (CP)). Then the duplexing/multiplexing and multiple access can be achieved at the same time by sharing all the subcarriers. Theoretically, each subcarrier can be assigned to any link. In practice, to mitigate the interference due to carrier frequency offset, a block of contiguous subcarriers (which we call a subchannel in the rest while its size may be different for different transmission schemes) can be taken as the allocation unit and some guard tones can be inserted if needed. In this paper, we do not consider guard tones. With proper synchronization, the isolation by large guard bands and time-switching among different links become unnecessary.

To illustrate the characteristics of the proposed MDMA scheme, we show examples of spectral resource assignments for MDMA, FDM-OFDMA and TDM-OFDMA in Fig. 1 for an M2M network with the number of nodes $N_x = 4$. Note that the actual resource assignments may be different depending on the scheduling scheme adopted. $\mathcal{L}_{k,l}$ denotes the link from node k to node l. For FDM-OFDMA, each node has its own transmission band and each band includes $N_x - 1$ subchannels for transmissions to the other $N_x - 1$ nodes. As shown in Fig. 1, guard bands are needed for FDM to separate different bands. For TDM-OFDMA, each node is assigned with one disjoint time slot out of every N_x time slots for transmission. Guard intervals are required between time slots to absorb propagation times and transmit-receive mode change interval. At its own time slot, each node occupies the whole band which is divided into $N_x - 1$ subchannels for transmissions to the other $N_x - 1$ nodes. Different from FDM-OFDMA and TDM-OFDMA, MDMA divides the overall spectrum into $N_x(N_x - 1)$ subchannels and can assign them disjointly to all links $\{\mathcal{L}_{k,l}\}$ without any constraints of the forward and reverse links being in different bands separated by guard bands or in different time slots separated by guard intervals. This yields more flexibility and gains in scheduling / resource allocation. Additionally, the proposed MDMA also makes it possible that multi-channel CSMA/CA is applied to M2M communication systems in a single (wider) frequency band with one transceiver for each node. On one hand, in MDMA, one transceiver is enough for a node to handle all the links. On the other hand, it may face with a large signal dynamic range problem, which we will discuss in the following.

B. Implementation Issues

1) Dynamic Range: In OFDMA-based P2M systems, we can address the dynamic range problem of the received signal by power control. However, in the proposed scheme for M2M communication networks, the dynamic range issue comes from both the leakage of transmission power to receiving subcarriers (transmission and reception happen simultaneously) and the near-far issue. Therefore, the dynamic range problem in the proposed scheme for M2M communication networks cannot be solved by conventional power control alone.

We consider the systems with small path loss range, e.g., wireless body area networks (WBAN) [17], intra vehicle networks [18], indoor power line communications [19], or pico / femto cells. In these systems, the path loss attenuation is relatively small. For example, in WBANs, the path loss can be less than 25 dB [17], and in indoor power line communications with 6MHz bandwidth over 150m communication distance, the path loss is around 25 dB [19]. In those systems, the dynamic range issue is no longer an obstacle for the implementation. Other potential application scenarios are inter-vehicle communications for safety and intelligent transportation, and advanced cellular systems where nearby mobile devices forming an M2M network for social or business interactions or gaming.

The dynamic range issue can also be addressed by the following approaches. To suppress leakage, an isolator with high attenuation can be adopted in the transceivers, e.g., an isolator with 85 dB attenuation in [20]. With a high attenuation isolator, the tolerance to the power differences between transmitted signals and received signals can be enhanced. To limit the dynamic range caused by multiple access, a scheme using an analog filter bank [16] and multi-band LNA [21] can be adopted. Therefore, with the existing technologies mentioned above, the proposed scheme can be implemented for those applications with small path loss attenuation. Improvements in isolator, filter bank, and LNA technologies will expand the coverage range and applications of the proposed scheme.

2) Cyclic Prefix: In OFDM/OFDMA, CP is used to avoid the inter-symbol interference and CP accommodates at least the maximum channel delay spread (T_{D}), timing synchronization errors, and the duration for time-domain windowing (to reduce the sidelobe interference to adjacent channels) [22]. Due to better time resolution of systems with wider bandwidth, MDMA and TDM-OFDMA can yield smaller timing synchronization errors and time-domain window duration than FDM-OFDMA. Without needing time-switching of TDM-OFDMA, MDMA could offer better fine timing synchronization via longer time averaging than TDM-OFDMA. While T_{D} is the same for all systems, MDMA additionally requires CP to cover propagation time since each node communicates with multiple nodes simultaneously. Depending on the deployment environment, CP requirement for MDMA varies. M2M networks typically aim at applications with short communication range (otherwise the randomly distributed nodes in M2M networks will experience significant near-far issues and RF front-end overloading, resulting in nonfunctional M2M networks) while the system may also support other non-M2M communications with a larger range. Thus, for M2M with short range, the effect of the propagation time on CP of MDMA can be neglected. For example, in IEEE 802.11a, the symbol duration is 4μs with 0.8μs guard interval [23]. If we consider 10m range for M2M, then 33ns more CP duration may be needed for MDMA and hence, from overhead perspective, it can be ignored compared with the 4 μs symbol duration. In wireline communications such as PoweRline Intelligent Metering Evolution (PRIME) protocol, CP is 192 μs while the symbol duration is 2.24ms [24]. If we consider 200m range for M2M, then MDMA may require 0.67 μs more CP duration which is also not significant. In addition, FDM requires large guard bands and TDM needs time switching (between TX and RX) guard intervals but those losses do not incur in MDMA. Overall, MDMA does not cause additional overhead for short range M2M communications.

3) Implementation Complexity: While MDMA and TDM-OFDMA require only one transceiver, FDM-OFDMA requires $N_x - 1$ receivers and one transmitter. This puts FDM-OFDMA at a disadvantage from cost and form-factor perspective.

Both MDMA and TDM-OFDMA require timing synchronization among different nodes but FDM-OFDMA does not. This implies lower complexity for FDM-OFDMA. But FDM-OFDMA receiver needs to always check whether signal has arrived or not. This offsets previous complexity advantage and increases energy consumption of FDM-OFDMA. Regarding frequency synchronization, each node of all schemes needs to estimate $N_x - 1$ carrier frequency offsets. Phase synchronization can be omitted as phase offsets can be absorbed into channel estimates. Channel estimation complexities for MDMA and TDM-OFDMA are the same as each receiver estimates the overall channels connecting to the other nodes. But for FDM-OFDMA, each receiver estimates partial bands of the overall channels connecting to the other nodes, thus its complexity is slightly lower. In terms of algorithms, existing synchronization and channel estimation methods for OFDMA (e.g., [25], [26]) can be appropriately applied to all schemes.

Compared with FDM-OFDMA and TDM-OFDMA, MDMA has more subchannels to schedule, thus incurring larger complexity and resource assignment overhead. However, compared with physical layer signal processing complexity, that of the scheduler is quite small. Consider the scheduler in Table I with N_{Link} active links and N_{ch} available subchannels (note: $N_{\mathrm{D}} = \min(N_{\mathrm{Link}}, N_{\mathrm{ch}})$). For all N_{Link} links to select their respective best subchannels, the complexity is $O(N_{\mathrm{Link}}N_{\mathrm{ch}})$. To resolve collisions in the subchannel selection, more rounds of selection are needed. In the worst case, we need $N_{\mathrm{D}} - 1$ rounds to schedule all subchannels. Therefore, overall the complexity is at most $O(N_{\mathrm{Link}}N_{\mathrm{ch}}N_{\mathrm{D}})$. Regarding scheduling overhead, MDMA requires $\lceil \log_2(N_x(N_x-1)) \rceil$ bits to assign a subchannel while FDM-OFDMA and TDM-OFDMA need $\lceil \log_2(N_x - 1) \rceil$ bits. Such additional overhead of MDMA is insignificant compared to its throughput gain as will be shown in Section V.

4) CSI Acquisition and Pilots Allocation: One of the advantages of the proposed MDMA scheme is its better capability and efficiency in obtaining CSI and adapting to the channels than the existing schemes. In MDMA, the transmitters can have CSI of the related links by exploiting channel reciprocity without requiring explicit CSI feedback. In addition, since the transmission is continuous, pilot tones

can be inserted in any symbol which means the CSI delay can be controlled. Different pilot sets of all transmitting nodes can be interleaved over the whole bandwidth. A common pilot set can be used for a transmitting node to all of its destination nodes. As shown in Fig. 2, the pilots for each node are uniformly spread over the whole frequency band (similar to pilots allocation in MIMO-OFDM, c.f., [27]), while the data for each link occupies a band-type (contiguous subcarriers forming a band or subchannel [28]). Depending on the channel length, pilot tones may occupy one or more OFDM symbols and they can be purely pilots or multiplexed with data. By this pilot design, every receiver can estimate not only the CSI of its data subchannel, but the whole frequency band of the connected links. By channel reciprocity, every node can have the CSIs of the reverse links. Simultaneously, the band-type data link can still enjoy substantial multiuser (multi-link) diversity gain via scheduling. Additionally, the density of the pilots can be adjusted according to the channel environment so that the pilot overhead and estimation accuracy are properly traded off. For channels with L taps each, the overall overhead for a CSI acquisition is LN_x tones.

In TDD/TDMA or TDM/OFDMA, owing to channel reciprocity, CSI feedback is not necessary, but CSI has some delay. For instance, as shown in Fig. 1, at node 1 the maximal CSI delay of $\mathcal{L}_{2,1}$ is the sum of transmission durations of node 3, node 4 and node 1 including the guard intervals. For time-varying channels, CSI may become substantially outdated. If the channel adaptation rate is kept the same, then MDMA and TDM-OFDMA have the same pilot overhead.

In FDD/FDMA or FDM/OFDMA, since the forward link and reverse link frequency bands are isolated from each other, explicit CSI feedback is required for CSI-based transmission schemes. Pilots (say L_1 tones) can be designed for each transmission band only (narrower than MDMA or TDM-OFDMA) and thus overall pilot overhead L_1N_x will be less. [1] During the CSI feedback (say analog feedback to maintain similar quality as in MDMA or TDM-OFDMA), for each band, $N_x - 1$ nodes need to send back analog CSI (i.e., $L_1(N_x-1)$ tones). Thus, the total overhead for CSI acquisition in FDM-OFDMA is $L_1N_x^2$ tones which is in fact larger than the overhead for MDMA and TDM-OFDMA.

III. MDMA with Centralized Scheduling

The proposed MDMA brings a larger scheduling gain via enhanced diversity under centralized access. To illustrate, we first study the performance of MDMA with a traditional scheduler. Then, we propose a more generalized paradigm in M2M networks by incorporating multicasting, and further explore MDMA's multicast throughput performance.

A. Traditional Scheduling Scheme

For an M2M network with N_x nodes, there are $N_x(N_x - 1)$ links. For example, a four-node M2M network has 12 links. Due to the channel reciprocity, there are $\frac{N_x(N_x-1)}{2}$ paired links

[1]For an OFDMA system with 256 subcarriers in a 12 tap channel described in Section V, a band with 60 subcarriers will need $L_1 = 6$ pilot tones (the rank of the corresponding channel covariance matrix based on its eigen values larger than 10^{-3} of the average of all eigen values).

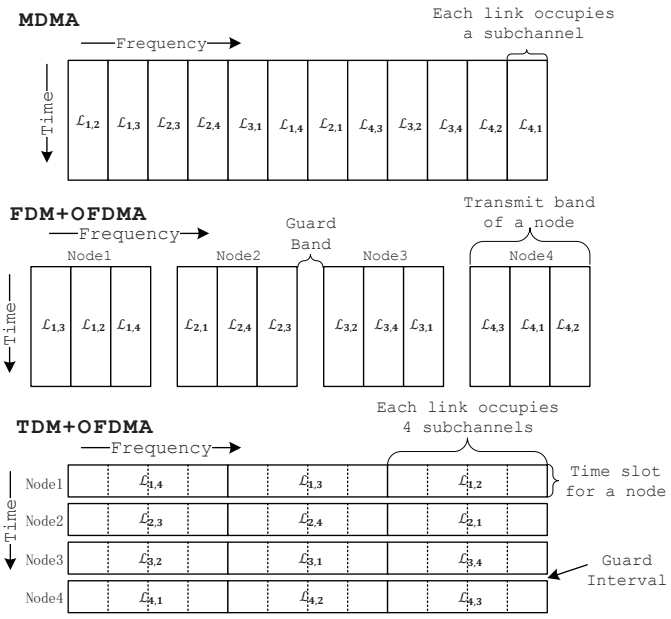

Fig. 1. An example of the resource assignments for different M2M schemes (The real assignments depend on the scheduling.)

and the forward and reverse links of each pair experience the same frequency-selective channel gains. In M2M networks, we can exploit CSI to capture multiuser/multi-link diversity via scheduling. We assume the central node has CSI of every link. Although optimal scheduling can be adopted, it incurs excessive amount of computation. To reduce the computation, we adopt a suboptimal scheduling scheme as described in Table I, since our purpose is just to illustrate the advantage of MDMA over the existing schemes using a practical scheduler.

TABLE I
Centralized Scheduling

Require: The channel power gain of each subchannel of each link $\{G_{k,l}(i)\}$.

while NOT all links have been assigned, **do**
  Select the best subchannel $\mathcal{I}_{k,l,\max}$ for each link.
  if $\{\mathcal{I}_{k,l,\max}\}$ are distinct **then**
    $\mathcal{I}_{k,l,\text{Assigned}} = \mathcal{I}_{k,l,\max}$
  else
    Assign the subchannel to the link with better channel power gain.
  end if
  Mark the assigned links and exclude all assigned links and subchannels from the remaining part of this algorithm.
end while

In the following, we explore analytical throughput performance for the MDMA with the above scheduler. We consider all multipath channels of different link pairs are mutually independent and identically distributed quasi-static Rayleigh fading channels. The overall spectrum is divided into $N_{\text{ch}} = N_x(N_x - 1)$ subchannels for MDMA as shown in Fig. 1. For analytical tractability, a simplified model is adopted for analysis as follows. We assume that the channel gains within each subchannel (composing of contiguous subcarriers) are the same (justified by setting the subchannel bandwidth to be smaller than the channel coherence bandwidth) and the channel gains of different subchannels are independent

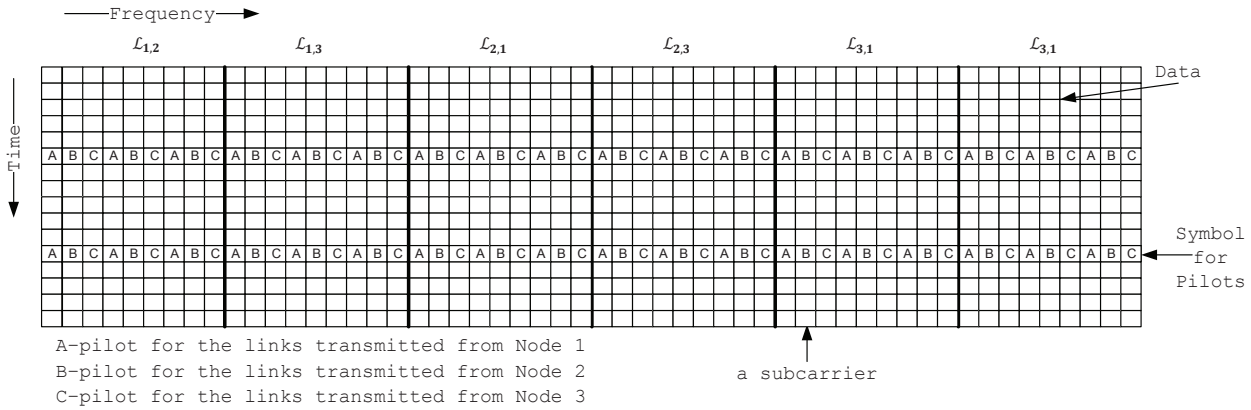

Fig. 2. An example of pilot allocation for MDMA in a 3-node M2M network.

(which will give an upperbound for our throughput analysis). The accuracy of the second assumption will improve with increased spacing between subchannels. For example, if the system has several M2M groups[2], then the subchannels of different groups can be interleaved in frequency and the above assumption is justified. Another scenario of justification is that the system reserves some spectrum resources for non-M2M applications and those resources can be interleaved with the M2M subchannels to provide better diversity gains to all.

In MDMA, each link is assigned with one of the subchannels. The maximum diversity order D of a link in the scheduling is the minimum of the channel diversity order and the number of subchannels $N_{\rm ch}$ of an M2M system. For the ease of comparison, we consider the scenario with $D = N_{\rm ch} = N_x(N_x - 1)$ for MDMA.

We denote the channel gain of the link $\mathcal{L}_{k,l}$ at ith subchannel as $H_{k,l}(i)$, where $H_{k,l}(i) \sim \mathcal{CN}(0,1)$ and denote the corresponding channel power gain $|H_{k,l}(i)|^2$ as $G_{k,l}(i)$ which is an exponential random variable with unit mean. The probability density function (pdf) and the cumulative distribution function of $G_{k,l}(i)$ are represented by $f_G(g)$ and $F_G(g)$. Consider N independent and identically distributed random variables $\{G_{k,l}(i)\}$. Let $\tilde{G}_{m,N}$ denote the mth order channel power gain of total N elements with $\tilde{G}_{1,N} \le \tilde{G}_{2,N} \le \ldots \le \tilde{G}_{N,N}$. Then the pdf of $\tilde{G}_{m,N}$ is given by

$$f_{\tilde{G}_{m,N}}(g) = \frac{N!\ F_G^{m-1}(g)[1-F_G(g)]^{N-m} f_G(g)}{(m-1)!(N-m)!} \quad (1)$$

$$= \frac{N!\ \left[1-e^{-g}\right]^{m-1} e^{-g(N-m+1)}}{(m-1)!(N-m)!},\ g \ge 0. \quad (2)$$

For a system with N subchannels, $N_{\rm s}$ subcarriers per subchannel and the average OFDM symbol rate R_0 at an average signal to noise ratio (SNR) of γ, the instantaneous throughput for $\mathcal{L}_{k,l}$ on its mth ordered subchannel is $C_{m,N} = R_0 N_{\rm s} \log_2(1+\gamma\tilde{G}_{m,N})$ and its average throughput is computed as (3), where $\mathrm{Ei}(x) \triangleq \int_{-\infty}^{x} \frac{e^t}{t} dt$ is the exponential integral function.

Due to channel reciprocity, i.e., $G_{k,l}(i) = G_{l,k}(i)$, the best a reciprocal link pair can obtain is that one of them is always assigned with its best subchannel out of $N_{\rm ch} = N_x(N_x-1)$ independent subchannels while the other link gets its second best. The corresponding average throughput of the system is

$$E[C_{\rm total}] = \frac{N_x(N_x-1)(E[C_{N_{\rm ch},N_{\rm ch}}] + E[C_{N_{\rm ch}-1,N_{\rm ch}}])}{2} \quad (4)$$

which represents an ultimate upperbound for any scheduler.

In practice, there are collisions in the subchannel selections of the links. A link would get its mth best subchannel ($(N_{ch}-m+1)$th ordered subchannel) with a non-zero probability q_m which will be very small for large m. We approximate the average throughput of the system as

$$E[C_{\rm total}] \approx N_x(N_x-1)\sum_{m=1}^{V} q_m E[C_{N_{\rm ch}-m+1,N_{\rm ch}}] \quad (5)$$

where the subchannels up to the V-th best (where $V \le N_{\rm ch}$) are included. For the scheduler in Table I, we derive upperbound analytical expressions for $\{q_m\}$ in the Appendix.

For FDM or TDM scheme, each node has $N_x - 1$ subchannels in its own transmission band or time slot for transmissions to the other $N_x - 1$ nodes (see Fig. 1). Thus, the diversity order in the scheduling for both FDM and TDM is $D = N_x - 1$, which is much less than MDMA. We will present throughput comparison of the three schemes in Section V-A.

B. Multicast Scheme with Optimal Scheduling

Here, we generalize the scheduling to allow more than one receiver for each transmission. By allowing multicasting in M2M systems, the resource scheduling offers more flexibility when two or more nodes require the same information. Consequently, system capacity can be further improved. We consider optimal scheduling with perfect CSI. For each transmission on a particular subchannel, a subset of receivers is selected such that the sum throughput is maximized. In other words, in multicasting, a subchannel can be assigned to several links originating from the same transmitting node.

We define a configuration to be a pair of transmitter-receiver(s). For example, in a four-node system, at each subchannel, there are a total of 28 possible transmitter-receiver configurations: $T_1 \to T_2$, $T_1 \to T_3$, $T_1 \to T_4$, $T_1 \to (T_2, T_3)$, $T_1 \to (T_2, T_4)$, $T_1 \to (T_3, T_4)$, $T_1 \to (T_2, T_3, T_4)$, $T_2 \to T_1$, $\ldots$, $T_4 \to (T_1, T_2, T_3)$. At each

[2]For K M2M groups, the system has $KN_{\rm ch}$ subchannels.

$$E[C_{m,N}] = R_0 N_{\rm s} \int_0^\infty \log_2(1+\gamma g) f_{\tilde{G}_{m,N}}(g) dg$$
$$= \frac{R_0 N_{\rm s}}{\ln 2} \frac{N!}{(m-1)!(N-m)!} \sum_{l=0}^{m-1} \frac{(-1)^{l+1}\binom{m-1}{l}}{l+N-m+1} e^{\frac{l+N-m+1}{\gamma}} {\rm Ei}\left(-\frac{l+N-m+1}{\gamma}\right) \quad (3)$$

subchannel, one of the 28 configurations is assigned. Denote the set of configurations as Ξ and its member as ξ.

Multicast achieves higher throughput by transmitting to possibly more than one receiver. But the transmission rate must be properly chosen to ensure all receivers being able to decode. For a single transmitter and a single receiver, the throughput of the configuration $T_k \to T_m$ on subchannel i is $R_0 N_s \log_2(1+\gamma G_{k,m}(i))$. For a configuration that has two receivers, the throughput must be limited by the channel of the weaker link to ensure successful decoding. Specifically, the throughput of the configuration $T_k \to (T_m, T_n)$ on subchannel i is $2R_0 N_s \log_2(1+\gamma \cdot \min(G_{k,m}(i), G_{k,n}(i)))$. The factor of two indicates double transmission rate from a single transmission to two receivers simultaneously. Similarly, the throughput of the configuration $T_k \to (T_m, T_n, T_o)$ on subchannel i is $3R_0 N_s \log_2(1+\gamma \cdot \min(G_{k,m}(i), G_{k,n}(i), G_{k,o}(i)))$. Let us drop the subchannel index i for simplicity and denote the instantaneous throughput of the configuration ξ as $C[\xi]$. For example, $C[T_k \to (T_m, T_n)] = 2R_0 N_s \log_2(1+\gamma \cdot \min(G_{k,m}(i), G_{k,n}(i)))$. Then the optimal scheduler selects the best configuration $\xi^\dagger$ for a subchannel as

$$\xi^\dagger = \arg\max_{\xi \in \Xi} \quad C[\xi] \quad (6)$$

which is easily obtained by computing $C[\xi]$ for all $N_x(2^{N_x-1}-1)$ configurations [29]. The signaling for resource assignment takes less than $N_x - 1 + \log_2(N_x)$ bits/subchannel.

A closed-form throughput expression is intractable due to intertwined involvement of order statistics of correlated and non-identically distributed random variables. Here, we propose an alternative way to approximate the average total throughput. From simulations, we found that the dominant configuration of multicast transmission is that one node transmits to all other $N_x - 1$ nodes. This configuration is more dominant at high SNR. Thus, we use this configuration in our analysis. For a given transmitter k on a subchannel, the related channel power gain G_k for computing throughput follows the minimum order statistics of order $N_x - 1$, i.e., the pdf of G_k is $f_{G_k}(g) = f_{\tilde{G}_{1,N_x-1}}(g)$. As the best out of N_x nodes is chosen, the corresponding channel power gain $\hat{G}$ of this subchannel is the maximum order statistics of $\{G_k : k = 1, 2, \cdots, N_x\}$ with the corresponding instantaneous throughput of $C = (N_x - 1)R_0 N_s \log_2(1+\gamma \hat{G})$. From the order statistics (c.f. (1)), the pdf of $\hat{G}$, $f_{\hat{G}}(g)$ with $g \geq 0$, is

$$f_{\hat{G}}(g) = N_x(N_x-1) \sum_{l=0}^{N_x-1} (-1)^l \binom{N_x-1}{l} e^{-(l+1)(N_x-1)g}. \quad (7)$$

Then, the average total throughput of MDMA is given by (8) which is expected to be an upper bound at high SNR since we assume independent subchannels. On the other hand, (8) will be a lower bound at low SNR since the transmission mode of one node transmitting to $N_x - 1$ is not dominant.

For FDM-OFDMA, consider that a group of consecutive subchannels is assigned to one particular node acting as a transmitter. Since there are total D subchannels, one group contains D/N_x subchannels. For each subchannel in this group, the configuration having the same node as a transmitter that maximizes throughput is chosen. Without loss of generality, let us assume node 1 (denoted T_1) as the transmitter. The number of configurations that need to be searched per group is $\binom{N_x-1}{1} + \binom{N_x-1}{2} + \ldots \binom{N_x-1}{N_x-1} = 2^{N_x-1} - 1$. The throughput averaged over subchannels in a group of FDM-OFDMA is

$$C = \frac{1}{(D/N_x)} \sum_{D/N_x \text{ subchannels}} \max_{\xi \in \Xi,\ T_1 \text{ is the TX}} C[\xi]. \quad (10)$$

The average total throughput $E[C_{\rm total}] = N_{\rm ch} E[C]$ is evaluated by simulation.

For TDM-OFDMA, all subchannels are assigned to the transmitting node. The number of configurations at each subchannel to be searched is similar to that of FDM-OFDMA per group. The instantaneous throughput is similar to MDMA with the condition of only one node (say T_1) acting as the transmitter. The instantaneous subchannel throughput is thus

$$C = \max_{\xi \in \Xi,\ T_1 \text{ is the TX}} C[\xi]. \quad (11)$$

Similar to FDM-OFDMA, the average total throughput $E[C_{\rm total}]$ is evaluated by simulation.

Table II summarizes the subchannel assignment algorithm with multicasting. This algorithm can be applied to all schemes, MDMA, FDM-OFDMA, and TDM-OFDMA.

TABLE II
OPTIMAL SCHEDULING WITH MULTICASTING

Require: The channel power gain of each subchannel of each link $\{G_{k,l}(i)\}$.

while NOT all subchannels have been assigned, **do**
  Select the best configuration that maximizes (6), (11) or (10) according to the multiple access scheme
  if More than one configuration is the best, **then**
    Randomly select one of them.
  else
    Assign the best configuration on this subchannel.
  end if
  Mark the assigned subchannels and exclude them from the remaining part of this algorithm.
end while

IV. DISTRIBUTED MDMA FOR M2M NETWORKS

Regarding OFDM-based distributed multiple access, there are two existing schemes, OFDM with single-channel CSMA/CA (e.g., 802.11a distributed coordination function (DCF)) and OFDMA with multi-channel CSMA/CA (e.g.,

$$E[C_{\text{total}}] = N_{\text{ch}}(N_x - 1)R_0 N_s E[\log_2(1+\gamma\hat{G})] \tag{8}$$

$$E[\log_2(1+\gamma\hat{G})] = \frac{N_x}{\ln(2)} \sum_{l=0}^{N_x-1} \frac{(-1)^{l+1}\binom{N_x-1}{l}}{l+1} e^{\frac{(l+1)(N_x-1)}{\gamma}} \text{Ei}\left(-\frac{(l+1)(N_x-1)}{\gamma}\right). \tag{9}$$

[12] which is only applied to the uplink of P2M networks). In M2M networks, to the authors' knowledge, OFDM with single-channel CSMA/CA is the only OFDM-based option used in the existing schemes. In this section, the multi-channel CSMA/CA is generalized to M2M networks. In addition, a new multi-channel CSMA/CA scheme which utilizes the local CSI is proposed here.

A. Multi-Channel CSMA/CA for M2M Networks

In [12], it is shown that the multi-channel CSMA/CA has two advantages over the single-channel CSMA/CA. First, the collision probability can be reduced. Second, the channel utilization can be improved by shortening the backoff time. Thus, the multi-channel CSMA/CA which is now generalized from P2M to M2M networks also helps the M2M networks to reduce the collision rate and improve the utilization of the channels, compared with the single channel CSMA/CA which is traditionally used in M2M networks.

We assume that ACK packets are transmitted by a dedicated error-free feedback channel as in [12]. Traditionally, OFDMA with multi-channel CSMA/CA is applied to the uplink and each node only sends packets to the base station. In M2M networks, each node may maintain several links simultaneously. To generalize the multi-channel CSMA/CA, we operate the protocol based on each link instead of each node. With random scheduling, we can modify the protocol for M2M networks as follows: A node with N_{link} (≥ 1) links waiting for transmission senses the activities of all the subchannels. If N_{ch} subchannels are idle for a period of DCF interframe space (a.k.a. DIFS in IEEE 802.11), then

- if $N_{\text{link}} \leq N_{\text{ch}}$, the node randomly selects and schedules N_{link} subchannels for N_{link} links.
- if $N_{\text{link}} > N_{\text{ch}}$, the node randomly selects and schedules N_{ch} links to transmit. The remaining $(N_{\text{link}} - N_{\text{ch}})$ links enter the backoff stage.

If there is no eligible idle subchannel, the node persists to monitor the subchannel until at least one subchannel is idle for a period of DIFS. At this point, those waiting links enter the backoff stage. In the backoff stage, each link generates a random backoff time independently before transmitting in order to reduce the collision probability.

The backoff stage in M2M scenario can be similar to that in the multi-channel CSMA/CA in [12]. The backoff time is uniformly selected from a contention window $[0, W-1]$. The window size W is initially set to the minimum value $W_{\min}$ at the first transmission attempt and obeys $W = 2^{N_{\text{bo}}-1}W_{\min}$, where N_{bo} denotes the number of backoff stages. The backoff counter is set to the backoff time which is determined above once the link enters the backoff stage. In a particular time slot, the backoff counter decreases by the number of eligible idle subchannels. A subchannel becomes an eligible idle subchannel when it is determined to be idle for a DIFS period. Once the backoff counter is down to zero, the link is activated to transmit the packet. Each link keeps its own backoff counter. If N_{link} links in a node activate at the same time (although its probability would be small), the random scheduler as described above is adopted. Thanks to the multi-channel feature, the multi-channel CSMA/CA maintains the advantages of lower collision rate and better channel utilization in M2M networks, which will be illustrated in Section V.

B. Multi-Channel CSMA/CA with Local CSI

In Section IV-A, we generalized the multi-channel CSMA/CA from uplink in P2M networks to M2M networks. However, the channel information, which could improve the throughput performance, was not considered in the protocol design. As described in Section II-B4, although it is a distributed system, each node can still estimate the channels over which it is communicating with other nodes. Especially, in slow fading channels, the local CSI can bring some throughput gain by means of channel selection and multiuser/multi-link diversity. Therefore, we propose a new scheme which utilizes the local CSI to improve the system performance.

Instead of the random scheduler adopted in Section IV-A, we adopt the maximum channel power gain scheduler. In practice, the number of subchannels would not be too large and thus the scheduler can search through all possible assignment combinations of subchannel and node pairs. An assignment combination $\mathcal{S}$ has $\min(N_{\text{link}}, N_{\text{ch}})$ different element pairs, and each element pair is a combination of an available subchannel index i and a destination node index l while different pairs contain different indexes. If the computation is of concern, then the scheduler in Table I or other efficient scheduler can be applied instead.

The scheduler can be described as follows:

- if $N_{\text{link}} \leq N_{\text{ch}}$, the node selects the N_{link} subchannels with the best assignment combination based on the channel power gain metric out of the N_{ch} subchannels for the N_{link} links and activates them at the same time slot.
- if $N_{\text{link}} > N_{\text{ch}}$, the node selects the N_{ch} links with the best assignment combination based on the channel power gain metric out of the N_{link} links and activates them at the same time slot.

For the kth node, the best assignment combination based on the power gain metric is defined as

$$\arg\max_{\mathcal{S}} \sum_{(l,i)\in\mathcal{S}} G_{k,l}(i). \tag{12}$$

In this scheduling, the best subchannel is assigned sequentially according to the adopted link activation order. Since different links at a node have different backoff stages, it is rare to have more than one link activated at a certain slot.

Thus, this scheduler is approximately the same as each link selects its best subchannel from the eligible idle subchannels. For links from different link pairs (a forward link and a reverse link count as a link pair), the channels can be considered as independent from each other. Thus, the collision probability among different link pairs would be the same as the random scheduler. For the link pair (forward and reverse links), due to channel reciprocity, the collision probability would increase. However, thanks to independent backoff stage, the probability that the two paired links activate simultaneously is low. Overall, the collision probability increase can be ignored, which will be verified in Section V.

The general analysis for the throughput appears to be intractable. Here, we consider a particular case that the two paired links are activated consecutively (e.g., when $\mathcal{L}_{1,2}$ is activated, $\mathcal{L}_{2,1}$ is also activated right after that, and vice versa). We denote the rth activated link as $\mathcal{L}_r$ (note: $r-1$ links have been already activated before it). In case of subchannels ordered by ascending channel power gains, the probability of link $\mathcal{L}_r$ taking the $\tilde{i}$th ordered subchannel is given as (13). Since the two paired links are activated consecutively, if r is odd, $\mathcal{L}_r$ is the first activated link in the pair while $\mathcal{L}_r$ is the second activated link in the pair if r is even.

We adopt the simplified model in Section III-A. By order statistics, the conditional pdf of the channel power gain given that the $\tilde{i}$th ordered subchannel is assigned to the considered link is $f_{\tilde{G}_{\tilde{i},D}}(g)$ given in (2) and the pdf of the channel power gain G_r of the rth activated link is $f_{G_r}(g) = \sum_{\tilde{i}=D-r+1}^{D} P_{r,\tilde{i}}\, f_{\tilde{G}_{\tilde{i},D}}(g)$.

The instantaneous throughput of $\mathcal{L}_r$ is given by $C_{\mathcal{L}_r} = R_0 N_s \log_2(1+\gamma G_r)$ and its average throughput is

$$E\left[C_{\mathcal{L}_r}\right] = \frac{R_0 N_s}{\ln 2} \sum_{\tilde{i}=D-r+1}^{D} \frac{D!\; P_{r,\tilde{i}}}{(\tilde{i}-1)!(D-\tilde{i})!} \sum_{k=0}^{\tilde{i}-1} \binom{\tilde{i}-1}{k} \times \frac{(-1)^{k+1}\; e^{\frac{D-\tilde{i}+1+k}{\gamma}}}{D-\tilde{i}+1+k} \mathrm{Ei}\left(-\frac{D-\tilde{i}+1+k}{\gamma}\right). \quad (14)$$

The total average throughput is given by

$$E[C_{\text{total}}] = \sum_{r=1}^{N_{\text{ch}}} E\left[C_{\mathcal{L}_r}\right]. \quad (15)$$

For random selection, the pdf of the channel power gain of each subchannel is exponential ($f_G(g)$) and hence its total average throughput is obtained as

$$E[C_{\text{total}}] = \sum_{r=1}^{N_{\text{ch}}} E\left[C_{\mathcal{L}_r}\right] = \frac{N_{\text{ch}} R_0 N_s}{-\ln 2}\; e^{\frac{1}{\gamma}}\; \mathrm{Ei}\left(-\frac{1}{\gamma}\right). \quad (16)$$

Comparison between (15) and (16) of the two schedulers will be presented in Section V together with simulation results.

V. Performance Evaluation

In deriving our analytical performance expressions, we adopted a simplified system where the channel gains of the subcarriers within each subchannel are the same but those of different subchannels are independent. However, in our simulation study in this section, we use a practical channel model, thus reflecting more practical performance. All schemes use the same quasi-static channel model with the same sampling frequency $(1/T)$ (i.e., N_F times the subcarrier spacing of TDM-OFDMA where N_F is the DFT size). Each channel includes T-spaced $L_0 = 12$ independent Rayleigh fading taps with 2 dB per tap decay factor in the power delay profile (PDP). All schemes use $N_F = 256$.

A. Centralized M2M Networks

We adopt a 4-node M2M network. For MDMA, all the 12 links equally share 240 subcarriers (the remaining 16 tones located at the band edges are guard tones). Due to channel reciprocity, there are entirely 6 pairs of independent channels. Within each pair, the channels are the same due to channel reciprocity. For TDM, we assume that at each time slot only one node can transmit while others are receiving. The transmission right is passed from one node to another at the end of each time slot. Thus, at any time slot, there are 3 links (each link occupies 80 subcarriers) transmitting simultaneously to 3 destinations, and the centralized scheduling approach is applied to these three links. For FDM, we assume there are 4 isolated frequency bands. Each band with 60 subcarriers is owned by one node to transmit data. Each band is equally shared by 3 links for 3 destinations where the centralized scheduling is applied. With the same channel model and sampling rate as in TDM-OFDMA and MDMA, FDM-OFDMA applies 4 times oversampling if compared with typical FDM. Different nodes of FDM-OFDMA use different disjoint sets of 60 contiguous subcarriers each as their respective transmission bands.

First, simulation results of throughputs for systems with the scheduler in Table I (without multicasting) are shown in Fig. 3(a). The proposed MDMA with centralized scheduling substantially outperforms all the other schemes. Due to better frequency diversity, TDM-OFDMA has a little bit better performance than FDM-OFDMA.

In Fig. 3(b), we compare analytical performance bounds and simulation results for MDMA with one M2M network as well as 4 M2M networks. For the case with 4 M2M networks (groups), each group has 3 nodes and each subchannel has 10 subcarriers (thus the same total amount of subcarriers as in one M2M network). The general upper bound (4) is rather loose but the bound (5) for the considered scheduler with $V = 7$ for one M2M network is about 1 dB SNR away from the simulation result while that with $V = 6$ for 4 M2M networks gives a close match. This verifies the validity of the simplified model adopted in our analysis.

To illustrate the overhead effect, we plot the performance results with and without overhead cost in Fig. 4. Here, scheduling is done for each packet of 15 OFDM symbols. The scheduling overhead is as in Section II-B3) and the pilot overhead is as in Section II-B4). As shown in Fig. 4, the impacts of overhead on each scheme as well as on relative performances of different schemes are insignificant.

Furthermore, in order to evaluate the impact of different path losses and shadowing among different links, we adopt the following model to simulate the combined effect of path loss and shadowing as $P(\text{dB}) = K + V$ where K is a constant for each link, V is a Gaussian random variable

$$P_{r,\tilde{i}} = \begin{cases} \frac{(r-1)!(\tilde{i}-1)!(D-r+1)}{(r-1-D+\tilde{i})!D!}, & 1 \le D-\tilde{i}+1 \le r < D, r \text{ is odd}, \\ \frac{(r-2)!(\tilde{i}-1)!(D-r+2)!(D-\tilde{i})}{D!(r-D+\tilde{i}-1)!(D-r)!}, & 1 < D-\tilde{i}+1 \le r \le D, r \text{ is even}, \\ 0, & \text{otherwise}. \end{cases} \tag{13}$$

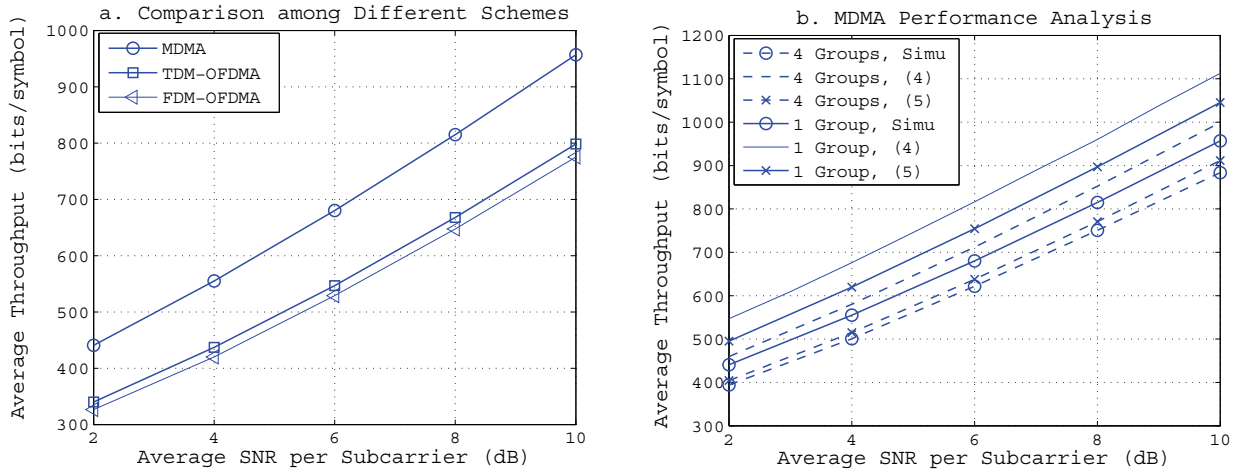

Fig. 3. Comparison of the average total throughput (normalized with $R_0 = 1$, thus equivalent to the average number of bits per OFDM symbol) for different scheduled access M2M networks.

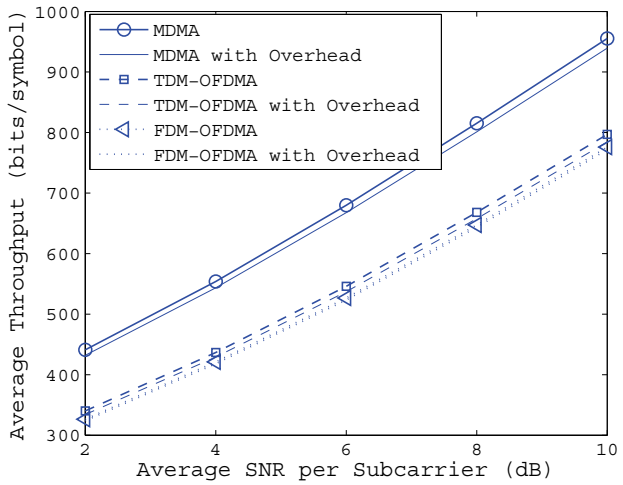

Fig. 4. Impact of overhead cost on throughput (normalized with $R_0 = 1$, thus equivalent to the average number of bits per OFDM symbol) for different scheduled access M2M networks.

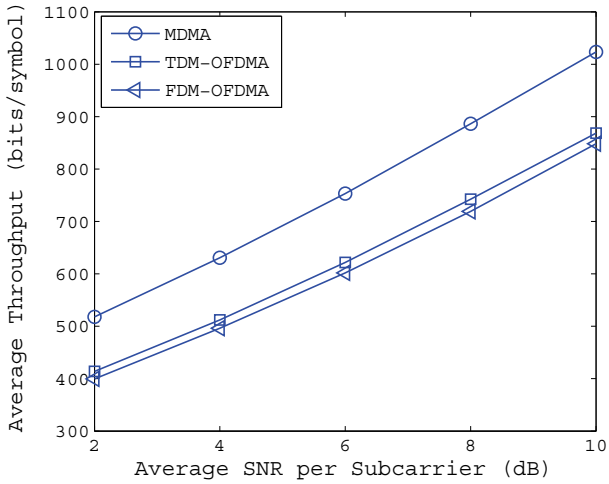

Fig. 5. Comparison of the average total throughputs (normalized with $R_0 = 1$) of different scheduled access M2M networks where the links are with different path losses and lognormal shadowing. Here, the average SNR is defined without path loss and shadowing.

(lognormal shadowing) and P is the combined effect of path loss and shadowing in dB. In simulation, we adopt $K = [-2, -2, -2, -5, -5, -5, 2, 2, 2, 8, 8, 8]$ (dB) and $V \sim N(0, 1)$. The performance result is shown in Fig. 5. We can observe that the proposed scheme sustains its substantial advantage over the existing schemes when considering the effect of different path losses and shadowing among the links.

Next, consider the multicast scheme under the same simulation setup and channel model. The subchannel assignment is performed to maximize transmission rate on each subchannel, subject to the multiple access scheme constraints. Note that each link is not constrained to only one source - one destination pair here. The simulation result for the throughput performance is shown in Fig. 6 together with the analytical result for MDMA (i.e., (8)). Higher gain of MDMA is achieved over TDM-OFDMA and FDM-OFDMA. We observe that FDM-OFDMA and TDM-OFDMA have almost the same performance here. Our analytical approximate throughputs closely match the simulation results. As expected, the analytical results slightly overestimate the throughput at high SNR and underestimate at low SNR.

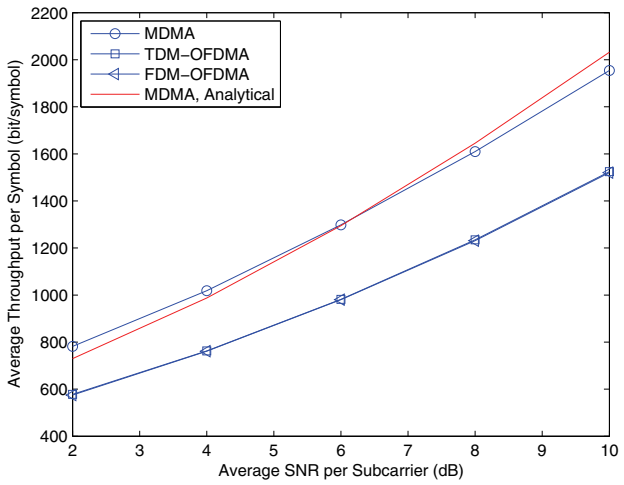

Fig. 6. Comparison of the average total throughput (normalized with $R_0 = 1$, thus equivalent to the average number of bits per OFDM symbol) for different scheduled access M2M multicast networks.

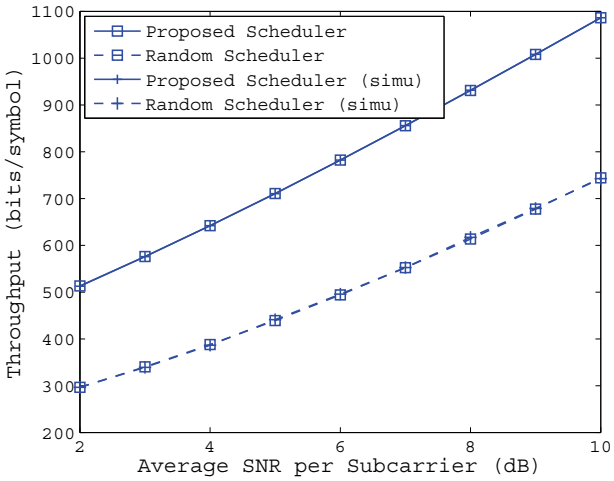

Fig. 7. Comparison of analytical and simulation average total throughput (average number of bits per OFDM symbol due to the setting $R_0 = 1$) between the proposed and random schedulers in a specific multi-channel CSMA/CA M2M network scenario.

B. Distributed M2M Networks

First, to verify the analytical throughput results ((16) and (15)) for the specific scenario of multi-channel CSMA/CA, we plot them in Fig. 7 together with their simulation results. Here, we assume there are 20 links and 16 independent subchannels, and each subchannel has 16 contiguous subcarriers. The analytical results match the simulation results for both schedulers. These results also confirm both analytically and by simulation that the proposed maximum channel power gain scheduler achieves a substantial throughput gain over the random scheduler by means of exploiting local CSI.

Next, we evaluate the proposed multi-channel CSMA/CA schemes in a general scenario by means of simulation. We adopt a 5-node network in which each node needs to communicate with all the other nodes. Therefore, there are 20 links. We set a time slot as an OFDM symbol of $50\mu s$. The transmission packet (frame) duration is 1.25ms for single-channel and $(1.25\text{ms} \cdot N_{\text{ch}})$ for multi-channel CSMA/CS schemes with N_{ch} channels (subchannels) in order to keep the same packet size per link in all considered schemes. The minimum contention window size $W_{\min}$ is 32, and the maximal number of backoff stages is $N_{\text{bo}} = 6$. For OFDMA, the DFT size and the number of used subcarriers are both set to 256. We select $256/N_{\text{ch}}$ consecutive subcarriers to form a subchannel. In the simulation, we consider the saturated throughput as in [12], where all the links have infinite data packets to transmit. The total average throughput is computed as

$$C_{\text{total}} = \sum_{k=1}^{N_{\text{ch}}} R_{\text{packet},k} E[C_{\text{packet},k}], \tag{17}$$

$$C_{\text{packet},k} = \frac{N_{\text{ch}} \cdot 1.25\text{ms}}{50\mu s} \sum_{i \in \mathcal{J}_k} \log_2(1 + \gamma G_k(i)), \tag{18}$$

where $G_k(i)$ is the channel power gain of the ith subcarrier in subchannel k with the subcarrier index set $\mathcal{J}_k$, $R_{\text{packet},k}$ is the average packet transmission rate (incorporating backoffs and collisions) and $C_{\text{packet},k}$ is the instantaneous throughput per packet on subchannel k. For single channel CSMA/CA, $N_{\text{ch}} = 1$ and hence $\mathcal{J}_1$ includes all subcarriers.

The simulation results for various channel access and throughput performances of single-channel CSMA/CA, multi-channel CSMA/CA without using local CSI and with local CSI in the considered M2M networks are shown in Figs. 8 and 9. We evaluate the network with the minimum contention window size $W_{\min}$ from 10 to 180 at 0 dB average SNR per subcarrier. The collision probability is shown in Fig. 8(a). Both of the two proposed multi-channel CSMA/CA schemes (without and with local CSI exploitation) give better performance than the traditional single-channel CSMA/CA. In our evaluation, more subchannels lead to lower collision probability, which illustrates that the multi-channel CSMA/CA in M2M networks keeps the advantage of low collision probability. Furthermore, the multi-channel CSMA/CA with local CSI has almost the same collision probability as the multi-channel CSMA with the random scheduler, confirming our discussion in Section IV-B.

Simulation results of the channel idle probability are shown in Fig. 8(b). With more subchannels, the idle rate reduces, which means the multi-channel CSMA/CA scheme can lower both idle probability and collision rate. But with a larger $W_{\min}$, the idle probability increases while the collision probability decreases. Thus, the selection of $W_{\min}$ is actually a trade-off between idle probability and collision probability. We also observe that the proposed schemes without and with local CSI exploitation yield practically the same idle probability.

Fig. 9(a) shows simulation results of the channel utilization rate defined as the ratio of successful transmission duration (subtracting collision duration and idle duration from overall duration) and overall duration. The proposed multi-channel CSMA/CA schemes obviously outperform the traditional single-channel CSMA/CA. The advantage of better channel utilization is still kept in M2M networks. The random scheduler and the maximal channel power gain scheduler give almost the same channel utilization rate. With the increase

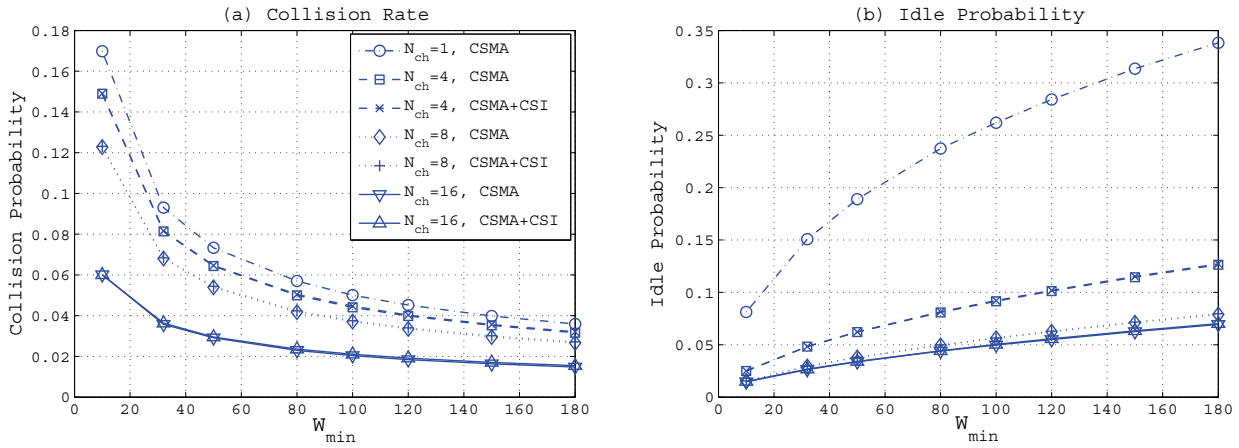

Fig. 8. Collision and idle probabilities of several distributed access schemes in an M2M network (same legend for (a) and (b)).

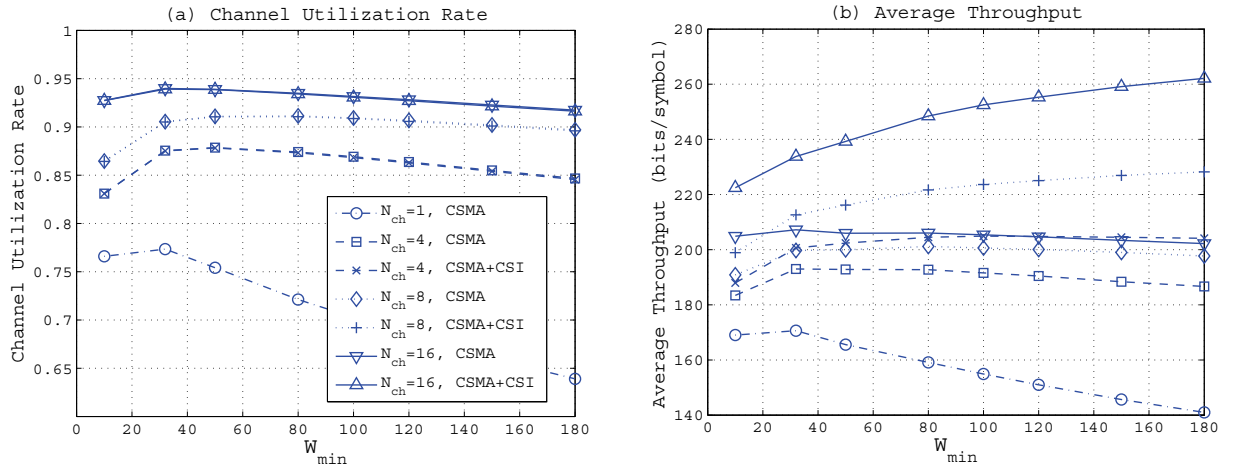

Fig. 9. Channel utilization rate and average throughput of several distributed access schemes in an M2M network (same legend for (a) and (b)).

of $W_{\min}$, the channel utilization rate first increases and then decreases. The reason is that a larger $W_{\min}$ can yield a lower collision probability while causing a longer idle duration.

The average throughput performance of several M2M distributed access schemes is shown in Fig. 9(b). The two proposed multi-channel CSMA/CA schemes are much better than the traditional scheme. With the same number of subchannels, the multi-channel CSMA/CA scheme utilizing local CSI obviously outperforms the one with the random scheduler. Especially, with more subchannels and a larger contention window size, the proposed scheme with the maximal channel power gain scheduler has more gain. If the number of subchannels and $W_{\min}$ are small, under the saturated traffic condition, the traffic will be still too crowded to be scheduled, and the scheduling gain will be limited in this case but the idle probability will decrease. When the number of subchannels and $W_{\min}$ become larger, although the idle duration may increase, the scheduling gain is also improved. In our evaluation, the scheduling gain brought by more subchannels and larger $W_{\min}$ is more significant than the increase of idle probability.

According to the simulation results, more subchannels can lead to better performance regarding collision probability, idle probability and channel utilization rate. Exploiting local CSI in the proposed scheme does not affect those performances but substantially enhances the throughput performance.

VI. Conclusions

We have proposed a new multi-point to multi-point (M2M) transmission scheme named multicarrier division multiple access (MDMA) which provides true M2M communications in the physical layer. MDMA handles duplexing/multiplexing and multiple access issues integratively while offering increased degrees of freedom and enhanced diversity in scheduling and resource allocation. We have presented existing as well as new scheduling algorithms for MDMA based M2M networks under both centralized and distributed access scenarios. We have also extended the functionality of the centralized M2M network by incorporating multicasting scenarios, and proposed the corresponding new M2M scheduler. Under the distributed access, we have generalized the traditional multi-channel CSMA/CA scheme of P2M networks for M2M networks, and proposed a new scheme which exploits local CSI and gives further performance gain. Closed-form analytical throughput expressions for both centralized and distributed access networks are also provided. Simulation results illustrate substantial throughput performance gains of the proposed schemes over the conventional ones in both of the considered centralized and random access scenarios. With the proposed

MDMA scheme, each node can handle all M2M links with only one transceiver for both centralized and multi-channel CSMA/CA networks, which is quite desirable from the size, cost and complexity perspectives.

APPENDIX

Here, we derive analytical expressions of $\{q_m\}$ for the scheduler in Table I. We divide $N_{\rm ch}$ links into two groups such that each group contains $N_{\rm ch}/2$ non-reciprocal links (the two groups are reciprocal). In the first step of scheduling, we can consider that $K_1(=N_{\rm ch}/2)$ links in the first group compete using their best subchannels over $N_1(=N_{\rm ch})$ subchannels. Suppose $\alpha_1 \in \{1,2,\cdots,K_1\}$ links are assigned with their best subchannels. In the second step, $K_2(=K_1)$ links from the second group compete using their best subchannels out of the remaining $N_2 = N_{\rm ch}-\alpha_1$ subchannels. Here, a link's contending subchannel can be anyone from its 2-nd to (α_1+1)-th best out of the original $N_{\rm ch}$ subchannels. Suppose this step assigns $\alpha_2 \in \{1,2,\cdots,K_2\}$ links of which $\alpha_{2,n}$ links obtain their nth best subchannels where $n \in \{2,\cdots,\alpha_1+1\}$ and $\sum_{n=2}^{\alpha_1+1}\alpha_{2,n}=\alpha_2$. In the ith step ($i \geq 3$), all the remaining K_i non-reciprocal links from both groups contend using their best subchannels out of the remaining $N_i = N_1 - \sum_{l=1}^{i-1}\alpha_l$ subchannels. For analytical tractability, we approximate K_i with an upper bound defined as the minimum of N_i and K_1. Suppose $\alpha_{i,n}$ links get their n-th best subchannels out of $N_{\rm ch}$ subchannels where $n \in \{i,i+1,\cdots,A_i\}$ with $A_i \triangleq 1+\sum_{l=1}^{i-1}\alpha_l$ and a total of $\alpha_i = \sum_{n=i}^{A_i}\alpha_{i,n}$ links are assigned in this step. The process continues with increasing i and stops when all the links have been assigned.

At the i-th step, a particular outcome α_i is contributed by a set $S^i_{\alpha_i}$ of corresponding distribution patterns $\{\Phi^i_{\alpha_i}\}$ of K_i links' contended subchannels. For example, for $\alpha_i = 2$ and $K_i = 6$, $\Phi^i_2 \in S^i_{\alpha_i}$ with $S^i_{\alpha_i} = \{[1,5],[5,1],[4,2],[2,4],[3,3]\}$. Then the conditional probability of a particular pattern $\Phi^i_k = [a_1,a_2,\cdots,a_k]$ given $\alpha_{[1:i-1]} \triangleq \{\alpha_n : n=1,\cdots,i-1\}$ and $\alpha_i = k$ reads as

$$P_{\Phi^i}([a_1,\cdots,a_k]|\alpha_{[1:i]}) = \binom{N_i}{k}\frac{K_i!}{N_i^{K_i}\prod_{l=1}^{k}a_l!} \tag{19}$$

and the conditional probability of $\alpha_i = k$ given $\alpha_{[1:i-1]}$ is

$$P_{\alpha_i}(k|\alpha_{[1:i-1]}) = \sum_{\Phi^i_k \in S^i_k} P_{\Phi^i}(\Phi^i_k|\alpha_{[1:i]}). \tag{20}$$

When $i=1$, (19) and (20) become unconditional probabilities.

At the first step, all α_1 assigned links have their best subchannels and hence the average number of links with the best subchannel is

$$\bar{\alpha}_1 = \sum_{k_1=1}^{K_1} k_1 P_{\alpha_1}(k_1). \tag{21}$$

At the step i (≥ 2), a subchannel assigned to a link can be any one from its i-th best to A_i-th best subchannels depending on what are available in the N_i subchannels. As the probability of an assigned subchannel being the m-th best subchannel with $m \in \{i,i+1,\cdots,A_i\}$ decreases as m increases, we will consider a maximum of three sequential orders, i, $(i+1)$, and $(i+2)$-th best subchannels in our analytical development. In other words, we will use $\alpha_{i,i}$, $\alpha_{i,i+1}$, and $\alpha_{i,i+2}$ but now $\alpha_{i,i+2}$ absorbs all $\{\alpha_{i,n} : n = i+2,\cdots,A_i\}$. At step i, the probabilities of a link's contended subchannel being its i-th, $(i+1)$-th, and $(i+2)$-th best subchannel are respectively given by $\rho_{i,i} = \frac{N_i}{N_1-i+1}$, $\rho_{i,i+1} = (1-\rho_{i,i})\frac{N_i}{N_1-i}$, and $\rho_{i,i+2} = 1-\rho_{i,i}-\rho_{i,i+1}$. We also assume for the analysis that any collided subchannel in the scheduling will be assigned to the link with the highest order statistics among the collided links. Then, we can compute the conditional expectation of $\{\alpha_{i,n}\}$ for $i \geq 2$ given $\alpha_{[1:i]}$ and $\Phi^i_k = [a_1,a_2,\cdots,a_k]$ as

$$\bar{\alpha}_{i,n}|_{\alpha_{[1:i]},\Phi^i_k} = \begin{cases} \sum_{l=1}^{k}\{1-(1-\rho_{i,i})^{a_l}\}, & n=i \\ \sum_{l=1}^{k}\{(1-\rho_{i,i})^{a_l}-(1-\rho_{i,i}-\rho_{i,i+1})^{a_l}\}, & n=i+1 \\ \alpha_i - \bar{\alpha}_{i,i}|_{\alpha_{[1:i]},\Phi^i_k} - \bar{\alpha}_{i,i+1}|_{\alpha_{[1:i]},\Phi^i_k}, & n=i+2. \end{cases} \tag{22}$$

Their unconditional expectation can be obtained as

$$\bar{\alpha}_{i,n} = \sum_{k_1=1}^{K_1}\cdots\sum_{k_i=1}^{K_i}\sum_{\Phi^i_k \in S^i_k}\bar{\alpha}_{i,n}|_{k_{[1:i]},\Phi^i_{k_i}} P_{\Phi^i}(\Phi^i_{k_i})P_{\alpha_1}(k_1) \cdot P_{\alpha_2}(k_2|k_1)\cdots P_{\alpha_i}(k_i|k_{[1:i-1]}), n=i,i+1,i+2. \tag{23}$$

To compute (5), we just need to compute the above for $i = 1,2,\cdots,V-2$. Then, the probability q_m that a link is assigned with its m-th best subchannel is given by

$$q_1 = \frac{\bar{\alpha}_1}{N_1}, \quad q_2 = \frac{\bar{\alpha}_{2,2}}{N_1}, \quad q_3 = \frac{\bar{\alpha}_{2,3}+\bar{\alpha}_{3,3}}{N_1}, \tag{24}$$

$$q_i = \frac{\bar{\alpha}_{i-2,i}+\bar{\alpha}_{i-1,i}+\bar{\alpha}_{i,i}}{N_1}, \ 4 \leq i \leq V-2, \tag{25}$$

$$q_{V-1} = \frac{\bar{\alpha}_{V-3,V-1}+\bar{\alpha}_{V-2,V-1}}{N_1}, \quad q_V = \frac{\bar{\alpha}_{V-2,V}}{N_1}. \tag{26}$$

REFERENCES

[1] A. Sentinelli, *et al.*, "Will IPTV ride the peer-to-peer stream? [peer-to-peer multimedia streaming]," *IEEE Commun. Mag.*, vol. 45, no. 6, June 2007, pp. 86–92.

[2] D. Schuster, T. Springer and A. Schill, "Service-based development of mobile real-time collaboration applications for social networks," in *Proc. 2010 Pervasive Computing Commun. Workshop*, pp. 232–237.

[3] S. Nasir, *et al.*, "Enhancing wireless video transmissions in virtual collaboration environments," in *Proc. 2007 Mobile Wireless Commun. Summit*, pp. 1–5.

[4] C. Diot, W. Dabbous, and J. Crowcroft, "Multipoint communication: a survey of protocols, functions, and mechanisms," *IEEE J. Sel. Areas Commun.*, vol. 15, no. 3, Apr. 1997, pp. 277–290.

[5] S. Konishi, Y. Kishi, and S. Nomoto, "Consideration on duplex modes and resource allocation algorithms for MP-MP BFWA networks carrying asymmetric traffic," in *Proc. 2002 IEEE WCNC*, pp. 774–779.

[6] I. F. Akyildiz and X. Wang, "A survey on wireless mesh networks," *IEEE Commun. Mag.*, vol. 43, no. 9, pp. S23–S30, Sept. 2005.

[7] A. Norman, "The ALOHA system: another alternative for computer communications," in *Proc. 1970 AFIPS – Fall*, pp. 281–285.

[8] X. Wang, "Throughput modelling and fairness issues in CSMA/CA based ad-hoc networks," in *Proc. 2005 IEEE INFOCOM*, vol. 1, pp.23–34.

[9] L. Xu, K. Yamamoto, and S. Yoshida, "Performance comparison between channel-bonding and multi-channel CSMA," in *Proc. 2007 IEEE WCNC*, pp. 406–410.

[10] J. Chen, S.-T. Sheu, and C.-A. Yang, "A new multichannel access protocol for IEEE 802.1 1 ad hoc wireless LANs," in *Proc. 2003 IEEE PIMRC*, vol. 3, pp. 2291–2296.

[11] D. Grace, A. G. Burr, and T. C. Tozer, "Comparison of a distributed dynamic channel assignment scheme with multichannel CSMA in a terrestrial radio environment," *IEE Proc. Commun.*, vol. 146, no. 3, pp. 191–195, Jun. 1999.

[12] H. Kwon, *et al.*, "Generalized CSMA/CA for OFDMA systems: protocol design, throughput analysis, and implementation issues," *IEEE Trans. Wireless Commun.*, vol. 8, no. 8, pp. 4176–4187, Aug. 2009.
[13] W. Qiu and H. Minn, "Orthogonal multicarrier division duplexing for point-to-point communications," in *Proc. 2012 IEEE ICC*, pp. 5479–5484.
[14] D. Steer, K. Teo, and B. Kirkland, "Novel method for communication using orthogonal division duplexing of signal (ODD)," in *Proc. 2002 IEEE VTC – Fall*, vol. 1, pp. 381–385.
[15] R. Kimura and S. Shimamoto, "A multi-carrier based approach to wireless duplex: orthogonal frequency division duplex (OFDD)," in *Proc. 2006 Intl. Symp Wireless Commun. Systems*, pp. 368–372.
[16] R. Kimura and S. Shimamoto, "An orthogonal frequency division duplex (OFDD) system using an analog filter bank," in *Proc. 2007 IEEE WCNC*, pp. 2275–2280.
[17] Y. Chen, *et al.*, "Cooperative communications in ultra-wideband wireless body area networks: channel modeling and system diversity analysis," *IEEE J. Sel. Areas Commun.* vol. 27, no. 1, pp. 5–16, Jan. 2009.
[18] R. D'Errico, L. Rudant, and J. Keignart, "Channel characterization for intra-vehicle WSNs in the ISM bands," in *Proc. 2010 European Conference on Antennas and Propagation*, pp. 1–5.
[19] M. Zimmermann and K. Dostert, "A multipath model for the powerline channel," *IEEE Trans. Commun.*, vol. 50, no. 4, Apr. 2002, pp. 553–559.
[20] C. R. Anderson, *et al.*, "Antenna isolation, wideband multipath propagation measurements, and interference mitigation for on-frequency repeaters," in *Proc. 2004 IEEE SoutheastCon*, pp. 110–114.
[21] A. Geis, *et al.*, "A 0.045mm^2 0.1-6GHz reconfigurable multi-band, multi-gain LNA for SDR," in *Proc. 2010 IEEE Radio Frequency Integrated Circuits Symposium*, pp. 123–126.
[22] J. Luo, W. Keusgen, and A. Kortke, "Optimization of time domain windowing and guardband size for cellular OFDM systems," in *Proc. 2008 IEEE VTC – Fall*, pp. 1–5.
[23] IEEE 802.11, "Wireless LAN medium access control and physical layer specifications."
[24] PRIME Alliance Technical Working Group, "Specification for PoweR-line Intelligent Metering Evolution," R 1.3.6.1.
[25] J. Zeng and H. Minn, "A novel OFDMA ranging method exploiting multiuser diversity," *IEEE Trans. Commun.*, vol. 58, no. 3, pp. 945–955, Mar. 2010.
[26] X. Fu, H. Minn, and C. D. Cantrell, "Two novel iterative joint frequency-offset and channel estimation methods for OFDMA uplink," *IEEE Trans. Commun.*, vol. 56, no. 3, pp. 474–484, Mar. 2008.
[27] H. Minn and N. Al-Dhahir, "Optimal training signals for MIMO OFDM channel estimation," *IEEE Trans. Wireless Commun.*, vol. 5, no. 5, pp. 1158–1168, May 2006.
[28] W. Qiu, H. Minn and C.-C. Chong, "An efficient diversity exploitation in multiuser time-varying frequency-selective fading channels," *IEEE Trans. Commun.*, vol. 59, no. 8, pp. 2172–2184, Aug. 2011.
[29] P. Tarasak and H. Minn, "Resource allocation for multipoint-to-multipoint orthogonal multicarrier division duplexing," in *2012 IEEE GLOBECOM*.

Wenxun Qiu (S'09, M'12) received the B.E. and M.S. degree in Electrical Engineering from Harbin Institute of Technology in 2005 and 2008. In 2012, he received the Ph.D. degree in electrical engineering from the University of Texas at Dallas. Currently, he is with Smart Grid Group in Texas Instruments Inc. His research interests include resource allocation in multicarrier systems, cognitive radio networks, advanced transmission schemes and smart grid communication technology.

Poramate Tarasak (S'97, M'05) received the B.E. degree in electrical engineering from the Chulalongkorn University, in 1997, the M.E. degree in telecommunications from the Asian Institute of Technology (AIT), Pathumthani, Thailand, in 1999, and the Ph.D. degree in electrical engineering from the University of Victoria, Victoria, BC, Canada, in 2004. From 2004 to 2005, he was a Postdoctoral Fellow with the Department of Electrical Engineering and Computer Science, KAIST, Daejeon, Korea. In 2006, he was a Researcher at NECTEC, Pathumthani, Thailand. From 2006-2013, he was a Research Fellow and a Scientist at the Institute for Infocomm Research, Singapore. Dr. Tarasak served as a TPC member for GLOBECOM 2013, 2012, ICC 2011 Workshop on HETnet, SmartGridComm 2012, PIMRC 2009, VTC Fall 2013, Fall 2012, Fall 2009. He was named as an Exemplary Reviewer for the IEEE WIRELESS COMMUNICATIONS LETTERS in 2012.

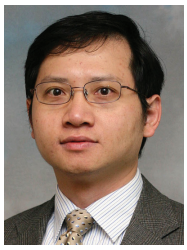

Hlaing Minn (S'99, M'01, SM'07) received the B.E. degree in electronics from the Yangon institute of Technology, Yangon, Myanmar, in 1995, the M.Eng. degree in telecommunications from the Asian Institute of Technology (AIT), Pathumthani, Thailand, in 1997, and the Ph.D. degree in electrical engineering from the University of Victoria, Victoria, BC, Canada, in 2001. He was a postdoctoral fellow at the University of Victoria during Jan.-Aug. 2002. He has been with the Erik Jonsson School of Engineering and Computer Science, the University of Texas at Dallas, Richardson since Sept. 2002, and currently is an Associate Professor. His research interests include wireless communications, statistical signal processing, error control, detection, estimation, synchronization, signal design, cross-layer design, cognitive radios, and wireless healthcare applications. Prof. Minn is an Editor for the IEEE TRANSACTIONS ON COMMUNICATIONS and *International Journal of Communications and Networks*. He served as a Co-Chair of the Wireless Access Track in the IEEE VTC 2009 (Fall) and TPC member in several IEEE conferences.